Monthly Notices
of the
ROYAL ASTRONOMICAL SOCIETY

Mon. Not. R. Astron. Soc. **415,** 2818–2826 (2011) doi:10.1111/j.1365-2966.2011.18899.x

Does stellar mass assembly history vary with environment?

Ben Hoyle,[1,2⋆] Raul Jimenez[1,3] and Licia Verde[1,3]

[1] *University of Barcelona (UB-IEEC), Marti i Franques 1, Barcelona 08024, Spain*
[2] *ICE & Consejo Superior de Investigaciones Cientificas, Serrano 117, Madrid 28006, Spain*
[3] *ICREA & Institute of Sciences of the Cosmos (ICC), University of Barcelona, Barcelona 08024, Spain*

Accepted 2011 April 11. Received 2011 March 23; in original form 2011 January 28

ABSTRACT

Using the publicly available VESPA data base of SDSS Data Release 7 spectra, we calculate the stellar mass weighted age (hereafter MWA) as a function of local galaxy density and dark matter halo mass. We compare our results with semi-analytic models from the public Millennium Simulation. We find that the stellar MWA has a large scatter which is inherent in the data and consistent with that seen in semi-analytic models. The stellar MWA is consistent with being independent (to first order) with local galaxy density, which is also seen in semi-analytic models. By splitting the sample into bins of total stellar mass, we find a strong dependence, with stellar MWA increasing for more massive galaxies.

As a function of increasing dark matter halo mass (using the SDSS New York Value Added Group catalogues), we find that the average stellar MWA for member galaxies increases, which is again found in semi-analytic models. We again split the sample into bins of total stellar mass, and still find a strong dependence on stellar MWA for increasing mass galaxies, but additionally a second order trend of increasing stellar MWA with increasing dark matter mass of the host halo.

Furthermore we use public dark matter mass accretion history (MAH) code calibrated on simulations, to calculate the dark matter MWA as a function of dark matter halo mass. In agreement with earlier analyses, we find that the stellar MWA and the dark matter MWA are anticorrelated for large mass haloes, i.e, dark matter accretion does not seem to be the primary factor in determining when stellar mass was assembled. This effect can be described by downsizing.

Key words: galaxies: evolution – galaxies: statistics – galaxies: stellar content.

1 INTRODUCTION

The spectra of galaxies encodes information about the histories of the component stellar populations, dust and star formation. Various tools have been developed to extract this information (e.g. Heavens, Jimenez & Lahav 2000; Tojeiro et al. 2007) and previous works have compared the resulting extracted information with both extrinsic and intrinsic galaxy properties. These approaches rely on the assumption that the evolution of the stellar populations are well understood and that the current modelling of stellar population is accurate.

The MOPED (Heavens et al. 2000) routine implements the general process of reforming a complex data set (e.g. a galaxy spectra) into a set of parameters [e.g. star formation rate (SFR), metallicity] and parameter combinations, assuming uncorrelated noise, such that the data compression is lossless (see also Graff, Hobson & Lasenby 2011). Mateus, Jimenez & Gaztañaga (2008) used MOPED-derived stellar masses and luminosities of SDSS Data Release 3 (Abazajian et al. 2005) galaxies to build marked correlations functions, and compared with marked correlations of semi-analytic models of galaxies in the Millennium Simulation.

More recently, Ferreras, Pasquali & Rogers (2010) applied a Principal Component Analysis technique, to decompose the spectra of low redshift ($z < 0.1$) SDSS early-type galaxies into two quantities: the average stellar age for the galaxy, assuming metal-rich stellar populations, and the fraction of recent star formation. They found little dependence (and a large scatter) of recent star formation and average stellar age on host halo mass, but find a stronger correlation on local processes, e.g. galactic velocity dispersion.

An easily accessible, robust code, is the VErsatile SPectral Analysis[1] (hereafter VESPA, see Tojeiro et al. 2007; Tojeiro et al. 2009, for more details) package, which recovers star formation and metallicity histories of the galactic spectra using synthetic stellar population

⋆E-mail: benhoyle1212@gmail.com

[1] http://www-wfau.roe.ac.uk/vespa/

models. The software recovers histories in adaptive age bins according to the signal-to-noise ratio of the galaxy spectrum on a case by case basis and addresses the age–metallicity relation. Two popular synthetic stellar population models are included in the VESPA output, those of Bruzual & Charlot (2003, hereafter BC03), and Maraston (2005) and Maraston et al. (2009) (hereafter M05), which differ in their respective resolutions, and the use of empirical libraries to model the thermally pulsating asymptotic giant branch. Furthermore VESPA corrects for galactic extinction using the dust maps of Schlegel, Finkbeiner & Davis (1998), and fits for the dust in each galaxy using either a one or two parameter dust model.

VESPA has been used by, e.g. Tojeiro et al. (2009) to compare the BC03 and M05 models, in particular, the recovered total stellar mass today (finds good agreement) and the mass averaged metallicity (finding less agreement). Tojeiro et al. (2011) used VESPA to model the colour evolution of high signal-to-noise ratio SDSS Data Release 7 LRGs as a function of colour, luminosity and redshift.

In this paper we compare the results of VESPA, in particular the epoch at which most of the stars were formed, the stellar mass weighted age (hereafter MWA), with similar results from *N*-body simulations and semi-analytic models. In particular we address the following questions.

(i) Does the stellar MWA depend on the local density?
(ii) Are similar trends seen in semi-analytic models?

To this end, we examine the correlation of local galaxy density with the VESPA calculated stellar MWA, and compare with the stellar MWA of the semi-analytic models in the Millennium Simulation (Springel et al. 2005; Boylan-Kolchin et al. 2009).

(iii) Is the stellar MWA correlated with the mass of the dark matter halo that the galaxy inhabits?

In this case, we match the galaxies used in VESPA with those from the New York Value Added Group catalogue (Blanton et al. 2005; Yang et al. 2007) and explore the average stellar MWA of member galaxies as a function of dark matter halo mass.

(iv) Is the stellar MWA correlated with the dark matter MWA?

We address this by comparing the results of the above analysis with the results of mass accretion history (MAH) code (Zhao et al. 2009), rebinned in terms of VESPA time bins for direct comparison to the observations.

VESPA uses the full galaxy spectrum to determine the ages of the component stellar populations and produce a stellar MWA. This is similar, but distinct from other galaxy age indicators, e.g. Gallazzi et al. (2005) who calculated the integrated *r*-band luminosity-weighted age for each galaxy spectra, by comparing different realizations of starburst models and their corresponding spectral line indices, with the observed galaxy spectra. This age estimate gives slightly more weight to the younger components of the stellar population, corresponding to more recent episodes of star formation, and thus are not directly comparable to the stellar MWA.

The layout of the paper is as follows: in Section 2 we describe the observational and simulated data and the process of reconstructing the stellar MWA of a galaxy. We continue in Section 3 by detailing our measurement of local galaxy density and dark matter halo mass, for both the observed and semi-analytic samples, and present the results in Section 4. We conclude and discuss in Section 5. Throughout the paper we employ a flat Lambda cold dark matter (ΛCDM) cosmology with (h, H_0, Ω_Λ, Ω_m, σ_8) given by (0.7, 100 $\times$ h km s^{-1} Mpc, 0.3, 0.8).

2 DATA

In this paper we compare observational data with semi-analytic models from simulations, and dark matter mass accretion code calibrated on dark matter simulations, and we describe all data sets below. We also include the Structure Query Language (hereafter SQL) commands to retrieve the data sets, and present the charateristics of the final data sets in Table 1.

2.1 Observed galaxy data

The 6 $\times$ 10^5 spectroscopically selected galaxies in this work were drawn from the Sloan Digital Sky Survey Data Release 7 (York et al. 2000; Abazajian et al. 2009, and references therein, hereafter SDSS DR7). Galaxy targets were selected from SDSS imaging and include

Table 1. A description of the data samples used in this work. We show the acronym used throughout this paper, the 'runid' from the VESPA data base applied to the SDSS DR7 spectra, the redshift cuts, and number of galaxies which have greater than four recovered VESPA age bins. We also show the galaxy data drawn from semi-analytic models retrieved from the Millennium Simulation, the redshift of output simulation, the number of galaxies and the number of parent haloes.

VESPA runs on SDSS D7 galaxy spectra			
Description	SP model and `runid`	Redshift range	Number of galaxies
Main Galaxy Sample (MGS)	BC03 2	$0.05 \leq z \leq 0.20$	594 326
LRG Sample (LRG)	BC03 6	$0.35 \leq z \leq 0.53$	25 334
Main Galaxy Sample (MGS)	M05 4	$0.05 \leq z \leq 0.20$	622 749
LRG Sample (LRG)	M05 8	$0.35 \leq z \leq 0.53$	75 423
Semi-analytic galaxies from the Millennium Simulation DeLucia 2006a table.			
Redshift	Number of galaxies	Number of parent DM haloes	
$z = 0.06$	21 155	7344	
$z = 0.12$	22 175	8272	
$z = 0.17$	21 818	8230	
$z = 0.36$	138	62	
$z = 0.41$	403	138	
$z = 0.51$	479	154	

'Main Galaxy Sample' (Strauss et al. 2002, hereafter MGS), and 'Luminous Red Galaxies' (Eisenstein et al. 2001, hereafter LRG).

Galaxy spectra were reprocessed using VESPA and we followed Tojeiro et al. (2009) in adopting the two parameter dust model. We note that our results are insensitive to the choice of dust models but are more sensitive (to within 20 per cent) to the choice of stellar population models, which we discuss in later sections.

We obtained the galaxy data using the following query run on the VESPA SQL web interface;[2] modifying the values of runid to obtain different dust models, stellar population models, and galaxy populations. We show the size of the galaxy samples obtained in Table 1 and describe the main parts of the query later in this section.

```
SELECT table3.indexP,table3.AgeMass/table3.TotMass AS MassWeightedAge,
table3.AgeZ/table3.TotZ AS ZWeightedAge,
table3.AgeSFR/table3.TotSFR AS SFRWeightedAge,
table3.TotSFR, table3.TotZ, table3.TotMass,
l.specObjID,n.redshift,d.dustval,d.runid, d.dustid,
n.m_stellar AS TotalCurrentStellarMass,n.nbins,
s.dered_g AS g,s.modelMagerr_g,s.dered_r AS r, s.modelMagerr_r,
s.dered_i AS i, s.modelMagerr_i, s.dered_z AS z, s.z AS spec_z,
s.zErr AS errspec_z, s.modelMagerr_z,
s.ra AS gal_ra, s.dec AS gal_dec,
s.MJD, s.FIBERID, s.PLATE, s.TILE, z.absMag_r

FROM (
    SELECT indexP, sum(mass*meanAge) AS AgeMass, sum(mass) AS TotMass,
    sum(Z) AS TotZ, sum(Z*meanAge) AS AgeZ, sum(SFR) AS TotSFR,
    sum(SFR*meanAge) AS AgeSFR
      FROM
        ( SELECT b.indexp, b.mass AS mass,
        (bID.ageStart+bID.ageEnd)/2 AS meanAge, b.Z, b.SFR

        FROM binprop AS b

        JOIN binID AS bID ON
        (b.binID = bID.binID AND b.runid = 8)

        JOIN lookupTable AS l ON (b.indexP = l.indexP)

     ) AS table2 group by indexp

   ) AS table3

JOIN lookupTable AS l ON (table3.indexP = l.indexP )
JOIN galprop n ON (table3.indexP=n.indexP AND n.runid=8)
JOIN dustprop d ON (table3.indexP=d.indexP AND d.runid=8 AND dustid=2)
JOIN bestDR7..SpecPhotoAll AS s ON (s.specObjID=l.specObjID )
JOIN bestDR7..photoz AS z ON (z.ObjID=s.ObjID )
```

In this work, we are concerned with one possible output of the VESPA data base, namely the stellar MWA. It is calculated, as in the above SQL query, as the sum over VESPA age bins i, of the mass M_i, formed in the bin, multiplied by the central bin age t_i, divided by the total stellar mass formed in the galaxy i.e.

$$\mathrm{MWA} = \frac{1}{M_{\mathrm{tot}}} \sum_i t_i M_i \ . \tag{1}$$

The adaptive binning inherent to VESPA adopts wide age bins for spectra with low signal-to-noise ratio, leading to an unnatural peak in the MWA distribution at 7 Gyr (which corresponds to the central value of the largest time bin, see Fig. 1 of Tojeiro et al. 2009). To remove these unphysical solutions we further imposed that the number of recovered VESPA bins is greater than 4, when determining averaged stellar MWA. We use the full data sets when calculating the local galaxy density. In Table 1 we present the final redshift ranges and the number of galaxies for both the MGS and the LRG samples using the different stellar population models.

2.2 Simulated galaxy data

The simulated data were drawn from the Millennium Simulation, which used a modified version of the collisionless dark matter and gas dynamical cosmological simulation code GADGET2 (Springel, Yoshida & White 2001; Springel 2005) with 2160^3 dark matter particles, each with mass $8.6 \times 10^8\, h^{-1}\, \mathrm{M}_\odot$, in a volume of side $500\, \mathrm{h}^{-1}$ Mpc. The simulation is able to recover dark matter haloes small enough to host luminous galaxies brighter than $0.1L_\star$.

The dark matter haloes were populated with galaxies according to the semi-analytic models of De Lucia et al. (2006) and De Lucia & Blaizot (2007). The models are novel in that they continue to follow dark matter haloes until they are tidally disrupted by parent haloes, and allow central galaxies to replenish their supply of cold gas, unlike satellite galaxies. They contain prescriptions for gas infall on to haloes, mixing between hot and cold gaseous states and cooling to form stars, and allow for cooling flows and their suppression by central galaxy Active Galactic Nuclei activity (see Springel et al. 2005; Croton et al. 2006; De Lucia, Kauffmann & White 2004, for specific details).

Both the galaxy properties and host dark matter halo properties are stored in the 'DeLucia2006a' table found on the public data access website.[3] We obtained information about local galaxy density, within a box of side $3h^{-1}$ Mpc centred on each galaxy, and the stellar MWA, using the below query.

```
SELECT d.galaxyID, d.haloID, d.stellarMass, d.snapnum, s.redshift,
s.lookBackTime, d1.galaxyID as galaxyid2 , d.massWeightedAge,
d1.massWeightedAge AS massWeightedAgeGal, d.centralMvir ,sdss.r_sdss

FROM DeLucia2006a d JOIN Snapshots s ON s.snapnum=d.snapnum
AND d.snapnum=60 JOIN DeLucia2006a d1 ON d.snapnum=d1.snapnum
AND d1.snapnum=60 AND ABS(d.x-d1.x) <1.5 AND abs(d.y-d1.y) <1.5
AND ABS(d.z-d1.z) <1.5 AND ABS(d.centralMvir - Msval) < 50
JOIN DeLucia2006a_SDSS2MASS AS sdss on d1.galaxyid=sdss.galaxyid
```

We called this query multiple times by looping over increasing values of 'Msval' to obtain all haloes with central halo dark matter mass within | d.centralMvir - Msval | < 50. This was performed to circumvent timeout errors. We chose to obtain data from the simulations with snap numbers 60, 58, 56, 51, 50, 48 which roughly correspond to the centres of the redshift bins used in the analysis which follows.

3 METHODOLOGY

In this section we describe the construction of the local galaxy densities and the assignment of dark matter halo masses to the observational and simulated semi-analytic data. We note that here the density is only dependent on cosmology through the volume element, which changes by less than 6 per cent (9 per cent) from $0.2 < z < 0.5$ in a flat fiducial ΛCDM when changing the cosmological parameter Ω_{m} from 0.3 to 0.25 (or h from 0.7 to 0.72).

3.1 Observational local galaxy density

The magnitude limits of the SDSS imply that we cannot directly compare the number density of all observed galaxies at different

[2] http://www-wfau.roe.ac.uk/vespa/SQL_form.html

[3] http://www.g-vo.org/Millennium

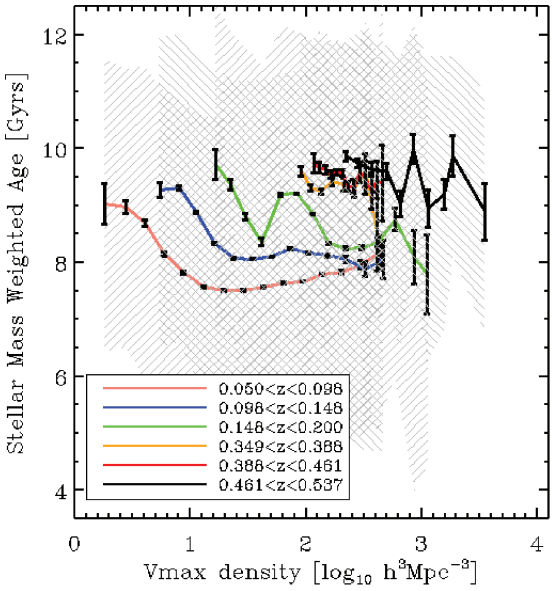

(a) BC03 model

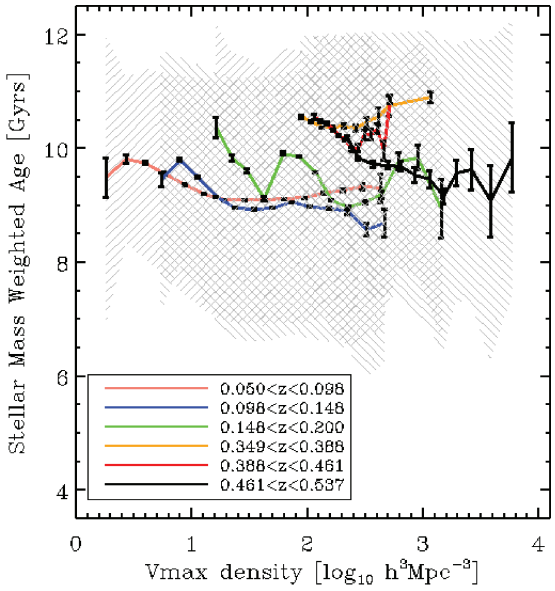

(b) M05 model

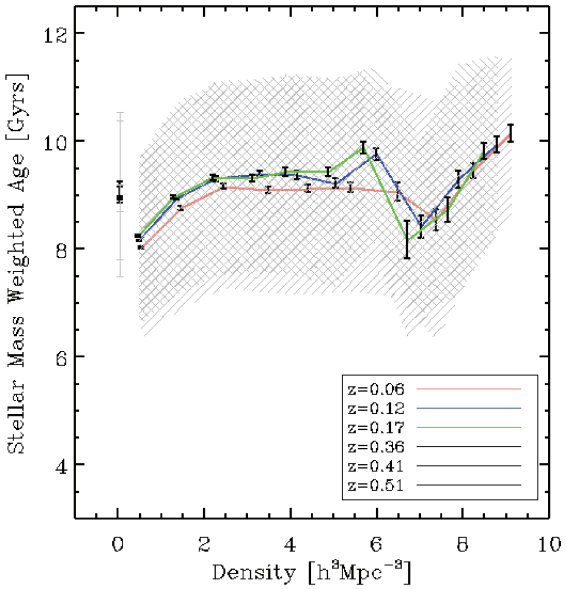

(c) SA model

Figure 1. The stellar MWA as a function of V_{max} weighted density, for SDSS galaxies. Fig. 1(a) shows the stellar MWA reconstructed using the BC03 stellar population models, and Fig. 1(b) uses the M05 models. Fig. 1(c) shows the stellar MWA of galaxies drawn from the Millenium Simulations by applying semi-analytic (SA) models to the dark matter haloes. The higher redshift LRGs and lower redshift MGS are each subdivided into three redshift bins, shown by the colour lines and black points. We show the 1σ standard deviation by the grey region, and the error on the mean by the black error bars.

redshifts. We therefore determined the maximum volume out to which each galaxy could have been observed, and weighted the density by this factor. This is the standard V_{max} correction (Schmidt 1968) and the maximum volume was calculated by spline fitting to the faint end of the band absolute magnitude M_r and redshift z distributions of the MGS and LRGs separately, using the line fitting package MPFITEXPR.[4] The equation of the spline fit is given by $z = 6.12 + 0.91M_r + 0.04\ M_r^2 + 7 \times 10^{-4}\ M_r^3$ with a chi-squared of 0.296, for the LRGs and $z = -262.22 - 31.52\ M_r - 1.26\ M_r^2 - 0.016M_r^3$ with a chi-squared of 0.780, for the MGS. We additionally removed galaxies fainter than the spline fit.

We calculated the local density in a cylindrical cell of radius $r_0 = 2.25h^{-1}$ Mpc (i.e. diameter $4.5\,h^{-1}$ Mpc) and length $l_0 = 4.5h^{-1}$ Mpc and additionally weighted each galaxy by its V_{max} correction. We also examined the effect on our results of changes in the cylinder volume, by modifying both the radius and length to $r_1 = 1.5$ and $l_1 = 3\,h^{-1}$ Mpc and $r_2 = 3$ and $l_2 = 6\,h^{-1}$ Mpc. We note that the dependence of stellar MWA with density for the LRGs using both stellar population models, are indifferent to the changes in the

[4] http://www.physics.wisc.edu/~craigm/idl/

cylinder volumes. We do, however, find that the stellar MWA for the MGS reduces slightly at higher densities (but stays within 1 Gyr) when examining smaller cylinders, but we do not find this effect to be significant. The effect is present for both stellar population models. Upon increasing the cylinder sizes, we find that the stellar MWA and density relationship remain unchanged.

Edge and survey holes were accounted for by creating a pixelized mask using the Hierarchical Equal Area isoLatitude Pixelization[5] (hereafter HEALPix Górski et al. 2005) routine, applied to a large SDSS DR7 photometric galaxy sample with resolution Nside=128, and only retaining pixels if they were completely surrounded by other pixels. At this HEALPix resolution there are many pixels per cylindrical cell. We divided the galaxy distributions into comoving distances slices such that there were three slices per cylinder length.

Each pixel in each redshift slice, which contained at least one galaxy became the centre of a cylinder (which itself spanned the redshift slice in front and behind of the redshift slice in question), within which we calculated the $V_{\rm max}$ weighted density for all galaxies in the cylinder (irrespective of the number of recovered VESPA age bins), and we further divided this by the total number of galaxies within the three redshift slices encompassing the cylinder. We then calculated the average stellar MWA of only the galaxies which resided in the central pixel.

3.2 Observationally estimated dark matter halo masses

We matched the SDSS DR7 galaxies in our sample to the group members catalogue (Yang et al. 2007) of the New York University Value-Added Galaxy Catalogue (NYU-VAGC; Blanton et al. 2005), which was run on the SDSS DR4 (Adelman-McCarthy et al. 2006) MGS. The group catalogue prescribes a dark matter halo mass to galaxy groups and clusters as a function of the total optical luminosity of galaxies above a characteristic luminosity (see Yang et al. 2007, for details). This optical-based dark matter halo mass was found to agree with the 'true' dark matter halo mass when compared with mock galaxy redshift surveys. For each dark matter halo, we calculated the mean of the stellar MWA of galaxy members.

As we were only able to estimate the dark matter halo masses of the low redshift MGS, we have restricted our comparison of the galaxies from the semi-analytic models, to the low redshift snapshots of the Millennium Simulation. We calculated the average stellar MWA of all galaxies in each parent dark matter halo.

3.3 Local galaxy density and halo masses from simulations

Using the SDSS data we determined the maximum absolute r-band magnitude of galaxies within each redshift slice, and applied the same absolute magnitudes cuts to the galaxies drawn from the semi-analytic models. These cuts were -16.24 for the three lower redshift snapshots, -22.66 for the higher redshift snapshots. The magnitude cuts applied to the higher redshift simulation outputs result in a lower number of recovered galaxies and haloes. The output of the SQL query returned the number of galaxies within a box of side $3\,h^{-1}$ Mpc centred on each galaxy. We then simply calculated the number of galaxies in each box which passed the absolute magnitude cuts and divided by the box size. We then recorded the stellar MWA of the galaxy at the centre of the box. We additionally calculated the average stellar MWA of all galaxies (which, again had passed the absolute magnitude cuts) in each parent dark matter halo.

[5] http://healpix.jpl.nasa.gov

4 RESULTS

4.1 Local galaxy density

In Fig. 1 we present the stellar MWA of VESPA galaxies using the BC03 and M05 models, as a function of $V_{\rm max}$ weighted density. We also show the stellar MWA of the semi-analytic model galaxies, as a function of local galaxy density at a range of redshifts chosen to coincide with the observed VESPA galaxies. The 1σ dispersion of the stellar MWA is indicated using the grey hashed regions, and the error on the mean by the black error bars. We show the median relations for each redshift by the coloured lines.

Both Figs 1(a) and 1(b) show that the SDSS MGS sample probe lower local densities than the higher redshift LRG sample, as expected from observations (e.g. Bamford et al. 2009).

We find that there is a large spread in stellar MWA as a function of $V_{\rm max}$-weighted density for both stellar population models with the VESPA data, and also find a similar stellar MWA dispersion for the semi-analytic models, see Fig. 1(c), although the density parameter has not been $V_{\rm max}$-corrected because the simulations are not magnitude dependent. Weighting the semi-analytic model galaxies by the $V_{\rm max}$ correction could add extra scatter.

We can try to understand if the large dispersion is actually a feature of the data, if it is due to systematic offsets in the stellar population models, or the noise in the galaxy spectra. Comparing the medians (the coloured lines) of the stellar MWA of the two different synthetic stellar population models run on the almost identical input data sets (the SDSS galaxies), we see that there is typically a 1–2 Gyr difference between them, which is indicative of a systematic offset. Additionally we can examine the results of Tojeiro et al. (2011), who stacked high signal-to-noise ratio spectra from the SDSS DR7 LRG sample (Abazajian et al. 2009), and compared VESPA outputs (e.g. redshift evolution of metallicity weighted age, MWA) between the BC03 and M05 models, see their fig. 6. They also find a $\gtrsim$20 per cent dispersion between the models, but also find that both models need to be modified to include additional error terms to fit the observed spectra well. These results suggest that the dispersion is at least partly due to the uncertainty in the models and systematic differences, independent of uncertainties in the data. If we now compare the dispersion to that seen in the galaxies drawn from the semi-analytic model, we conclude that the remaining scatter is a combination of being intrinsic to the data and due to noise.

Examining Figs 1(a) and 1(b) we see that, as noted above, the two different stellar population models agree to within $\sim$20 per cent, and that in both cases there is a $\sim$1-Gyr difference between the stellar MWA of LRGs and MGS, which is a consequence of an older stellar population, i.e. there has been comparatively little or no recent star formation in LRGs compared with MGS. We note that a direct comparison of the BC03 and M05 stellar MWA for the 21801 LRG galaxies with measured stellar MWA and the constraint $Nbins > 4$ has a large scatter (68 per cent = 3.7 Gyr) and a small systematic offset of 0.6 Gyr. A possible explanation of the systematic offset, is that, of the two stellar population models used in VESPA, the M05 had a lower wavelength resolution than BC03. VESPA rebins the data to the models, so the signal-to-noise ratio is larger in the M05 models, and thus more age bins are recovered. Also there is a decrease in star formation between 0.1 and 1 Gyr using BC03, which will mean there will be little stellar mass assembled in the corresponding VESPA age bins, i.e. the stellar MWA will be skewed lower than the M05 models. Panter et al. (2007) used SDSS DR3 galaxies and examined the effect on the recovered SFRs of different stellar population models (BC03, M05 and others), and model resolutions.

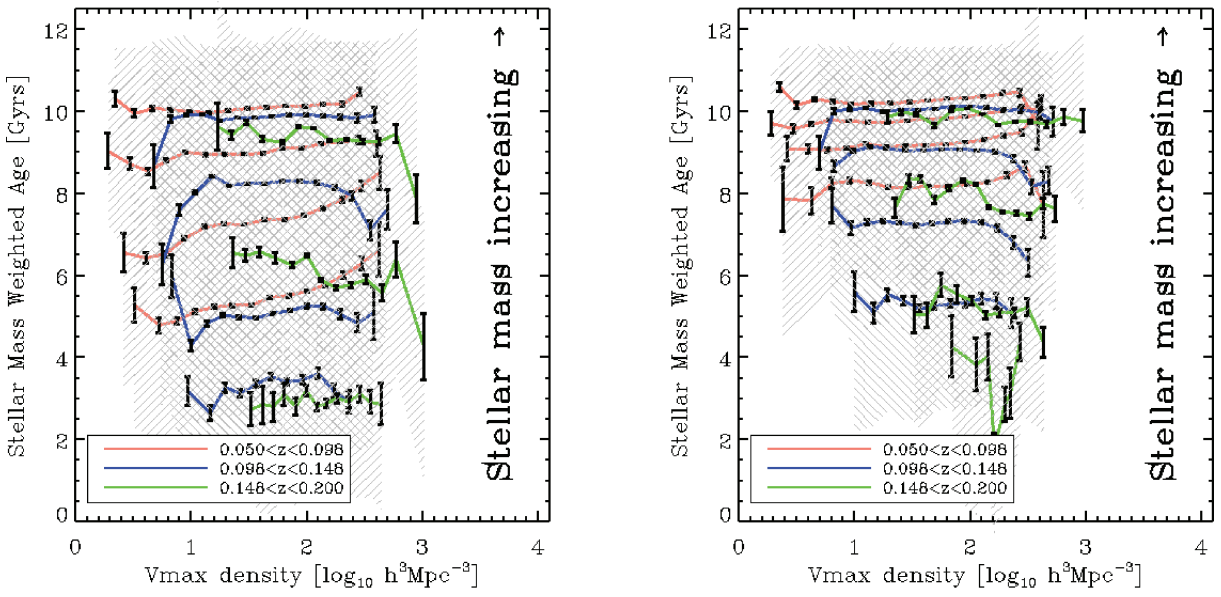

(a) BC03 (b) M05

Figure 2. The stellar MWA and V_{max} weighted density relation of the low-redshift MGS, subdivided into bins of total stellar mass for the BC03 model (left-hand panel) and M05 model (right-hand panel). We use the coloured lines to distinguish redshift slices, and like coloured lines of increasing stellar MWA correspond to bins of increasing total stellar mass. The stellar mass M bins are given in units of $M_{\odot}$, by the ranges $10.2 \leq \log_{10} M < 10.4$, $10.4 \leq \log_{10} M < 10.8$, $10.8 \leq \log_{10} M < 11.2$ and $11.2 \leq \log_{10} M < 11.6$, and split the sample into bins of roughly equal number. The error on the mean is again shown by the black error bars, and the 1σ dispersion by the grey hashed region.

They found a <30 per cent systematic difference in the recovered SFRs when changing model resolution, and identified a ∼10 per cent systematic offset between stellar population models. We also note that the M05 (BC03) stellar population models recover stellar MWA below 5 Gyr for ∼4 per cent (∼10 per cent) of LRGs. This could be due contamination of non LRGs in the LRG sample, or by limitations in the stellar population models.

Continuing to examine Figs 1(a) and 1(b) we also find that the stellar MWA for all galaxies is typically older than 8 → 9.5 Gyr in look-back time for the MGS, and typically older than 9 → 10 Gyrs for the LRGs. We note that Fig. 1(c) is divided by redshift, but does not distinguish between LRG and MGS galaxy populations (i.e. they are combined here), but do produce the same trends, i.e. that the largest fraction of stellar assembly occurred before 8-Gyr look-back time.

For each galaxy sample analysed with the BC03 model, we find that the median stellar MWA of the three increasing redshift slices increases. This suggests that even though the majority of star formation occurred at high redshift, both the LRG and MGS samples continuously have small amounts of stars being assembled, thereby reducing their stellar MWA. This effect is less apparent with the M05 model, with only the two upper redshift slices of the MGS obeying this trend.

This weak trend is, however, consistent with observations of the continual SFRs (SFR) of both low and high mass galaxies across cosmic time (Conroy & Wechsler 2009; Noeske et al. 2007a,b, although note that the SFR for high-redshift massive galaxies is greater than for high-redshift low-mass galaxies).

All panels of Fig. 1 appear to show no, or little dependence of stellar MWA on local galaxy density to first order. Also note that the observed and simulated trends agree with each other within the dispersion. Furthermore, we see no discernible trends between the different redshift slices of either the MGS or LRGs as a function of density.

A correlation of very local galaxy density (related to projected density of the 5 th nearest neighbour, Cooper et al. 2005) and galaxy age estimates following Gallazzi et al. (2005) have led Cooper et al. (2010) to find a strong relation between galaxy age and local galaxy density at fixed stellar mass. Our estimates of density are in much larger volumes, and thus these smaller scale correlations are smoothed out.

In Fig. 2 we have split the stellar MWA and V_{max}-weighted density relation into bins of total stellar mass for both models. We use the coloured lines to distinguish redshift slices, and like coloured lines of increasing stellar MWA correspond to bins of increasing total stellar mass. The stellar mass M bins are given in units of $M_{\odot}$, by the ranges $10.2 \leq \log_{10} M < 10.4$, $10.4 \leq \log_{10} M < 10.8$, $10.8 \leq \log_{10} M < 11.2$ and $11.2 \leq \log_{10} M < 11.6$, which split the sample into bins of roughly equal galaxy number. The error on the mean is again shown by the black error bars, and the 1σ dispersion by the grey hashed region. We have only shown the mass splitting of the lower redshift MGS to make the figures more readable. There is very little stellar MWA splitting between the bins of equal mass for each redshift slice of the LRG sample.

The stellar MWA is consistent with being independent on local galaxy density, independent of total stellar mass bin, redshift slice or stellar population model, within the 1σ spread of the data. However, we do find that the stellar MWA of lower mass galaxies is consistently lower than more massive galaxies, across all redshift slices and independent of the stellar population model. This suggests that the lower the mass of a galaxy, the more stellar mass is assembled at late times, i.e. low-mass galaxies are younger than high-mass

galaxies. This result has been observed before, e.g. Jimenez et al. (2005), Panter et al. (2007) found that the SFRs of massive galaxies peaked earlier than less massive galaxies.

4.2 Dark matter halo mass

We now compare both the stellar MWA (for low-redshift galaxies matched to the DR4 NYVAC group catalogue) and the dark matter MWA, to the dark matter host halo mass. To do so we used the publicly available code of Zhao et al. (2009) which calculates the MAH of dark matter haloes back through cosmic time, by assuming that the progenitor of a halo is always the most massive of all progenitors. The fitting formula was calibrated on suites of N-body dark matter simulations (see Zhao et al. 2009, for details) and was found to be accurate to within $\lesssim$5 per cent and universal. Results may be defined in terms of M_{200}, which enabled direct comparison with the halo masses of the NY VAC group catalogue.

In Fig. 3(a) we show, as a function of halo mass, the percentage of accreted dark matter on to the dark matter haloes per time interval, relative to the halo mass at $z = 0$. The black lines show the time steps as outputted by the MAH code, and the red lines show different realizations of the larger time steps corresponding to a random selection of >4 VESPA age bins. The VESPA age bins were chosen by imposing the constraint that each random sample of bin selections be consecutive and complete across the full VESPA time range. This age bin selection was performed to most closely match the conditions of the VESPA data; recall that each included galaxy spectrum has a high signal-to-noise ratio, such that VESPA could determine stellar histories in >4 different age bins. The different line styles correspond to different mass haloes at $z = 0$.

Fig. 3(b) shows the stellar MWA as a function of dark matter halo mass, as measured from galaxies using semi-analytic models in the Millennium Simulation. We note that the masses probed by the simulations is lower than those from the NYVAC, but we do see a clear increase in the stellar MWA with increasing dark matter halo mass, in agreement with the VESPA data, and again opposite to the trends seen in the dark matter MWA, as seen by the blue contours in the lower panels of Fig. 3.

In Fig. 3(c) we show the average stellar MWA of halo member galaxies as a function the dark matter group halo mass, and distinguish between the M05 models (red) and BC03 models (green). We show the 1σ dispersion by the grey hashed region, and the error on the mean by the black error bars. We again note that the spread of data is large, and that the models agree to within $\sim$1.5 Gyr. For both models we see a slight increase in the stellar MWA for increasing dark matter halo mass, which suggests that more massive groups and clusters formed the majority of their stars earlier in the Universe's history than less massive groups, or similarly, that stellar mass was still being assembled in lower mass groups more recently. We additionally show the dark matter MWA by the black dotted line. The blue contours correspond to 10^4 dark matter MWA measurements drawn from random samplings of the 30 VESPA age bins, with the constraints (as introduced above), that we randomly choose more than four VESPA bins, and that the bins form a full and continuous coverage of VESPA ages. We see that the dark matter MWA becomes lower as the group mass increases, and that the 1σ simulated dispersion is constant as a function of group mass.

The stellar and dark matter MWA of the smaller systems have similar values, but this may not be a physical correlation because of the anticorrelation of the stellar and dark matter MWA at higher masses. This leads us to infer, that while the stellar MWA is correlated with the overall mass of the dark matter halo, is it not correlated with the accretion of dark matter on to the halo.

We finally present Fig. 3(d), which is the same as Fig. 3(c), but split into bins of total stellar mass M, as before the bins are given in units of $M_\odot$, by the ranges $10.2 \leq \log_{10} M < 10.4$, $10.4 \leq \log_{10} M < 10.8$, $10.8 \leq \log_{10} M < 11.2$ and $11.2 \leq \log_{10} M < 11.6$, which split the sample into bins of roughly equal galaxy number. The error on the mean is again shown by the black error bars, and the 1σ dispersion by the grey hashed region.

We find that for galaxies with lower stellar mass, there is a sharp decrease in the stellar MWA between dark matter group masses of $5 \times 10^{11} < M < 5 \times 10^{12}\, h^{-1}\, M_\odot$ and then a gradual increase in stellar MWA as group halo mass increases. This could be indicative of small mass haloes ($M \sim 5 \times 10^{11}\, M_\odot$) exhausting their supply of gas to convert to stars early-on, but processes such as feedback at slightly higher halo mass ($M \sim 10^{12}\, M_\odot$) allowing gas to cool later, causing more recent star formation, and thus decreasing the stellar MWA. As the halo mass increases, the stellar MWA for galaxies then increases, as expected in the downsizing scenario.

At higher stellar mass, we find no dependence between stellar MWA and group halo mass within the dispersion. This suggests that, as before, stellar mass is the dominant component of determining the stellar MWA, with second order effects dependent on the host halo mass. This relationship has been seen by Pasquali et al. (2010) who examined the relationship between SDSS galaxy r-band luminosity weighted ages of Gallazzi et al. (2005) with increasing halo mass. They distinguish central and satellite galaxies and find that for lower mass galaxies, the galaxy age increases as the halo mass increases, but that this trend is reduced as stellar mass increases. They also find that the dominant contribution to changes in the galaxy age is total stellar mass.

5 CONCLUSIONS

We used the results of VESPA (Tojeiro et al. 2007, 2009) which analysed 10^6 SDSS DR7 (Abazajian et al. 2009) galaxy spectra, to calculate the stellar MWA. To remove peculiarities in the data, we chose to only use high signal-to-noise ratio spectra which allowed the measurement of stellar histories in greater than four VESPA age bins. We then calculated the local galaxy density of the all the SDSS galaxies in cylinders of radius $2.25\, h^{-1}$ Mpc and length $4.5 h^{-1}$ Mpc, and applied the standard $V_{\rm max}$ correction to account for the magnitude limits of the SDSS. We also cross-matched the VESPA galaxies with the New York Value Added Group Catalog (Yang et al. 2007), which includes estimates of the parent dark matter halo mass.

Using the public code of Zhao et al. (2009), we determined the dark matter MWA as a function of halo mass. We additionally obtained the stellar MWA, local galaxy density, and dark matter halo masses of galaxies from within the Millennium Simulation (Springel et al. 2005), populated according to the semi-analytic models of De Lucia et al. (2006).

We found a large scatter in the recovered stellar MWA, which we determined to be partially due ($\sim$20 per cent) to the differences between the BC03 (Bruzual & Charlot 2003) and M05 (Maraston et al. 2009) stellar populations models, by comparing the medians of our distributions, and also by examining the results of Tojeiro et al. (2011), who compared the differences between models when applied to stacked LRG spectra with high signal-to-noise ratio. A large dispersion is also observed in the stellar MWA of the semi-analytic models, suggesting that the dispersion is also inherent to the data. We found that the recovered stellar MWA using the

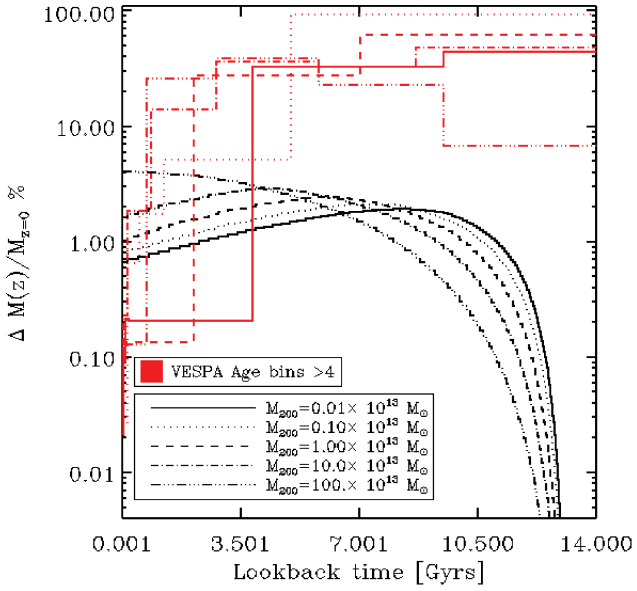

(a) Dark matter MAH

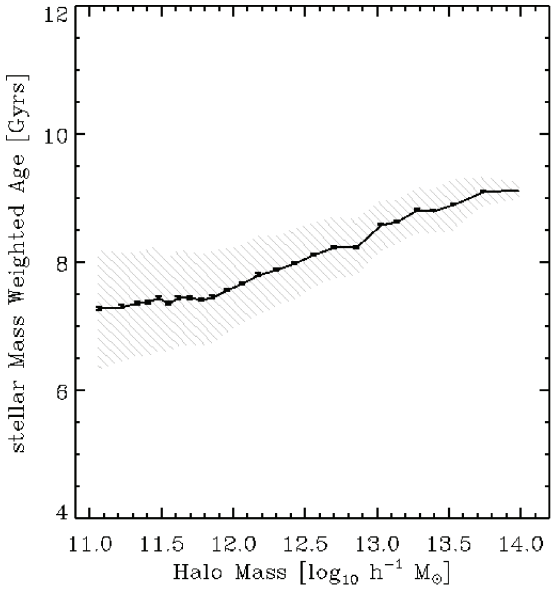

(b) Semi analytic models

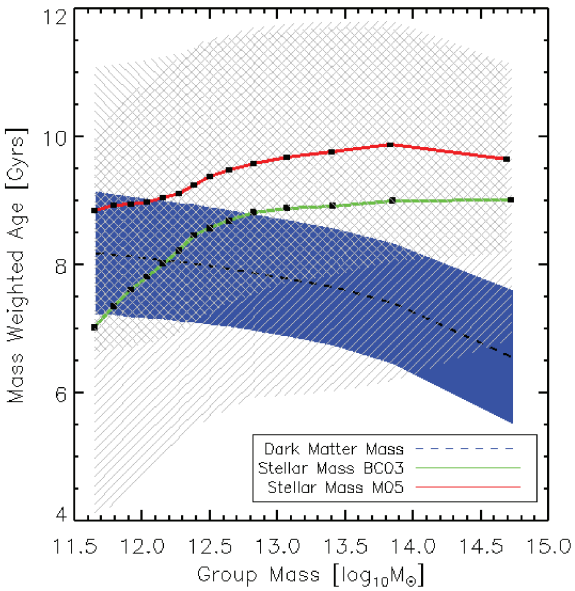

(c) BC03 & M05 models, with DM MWA

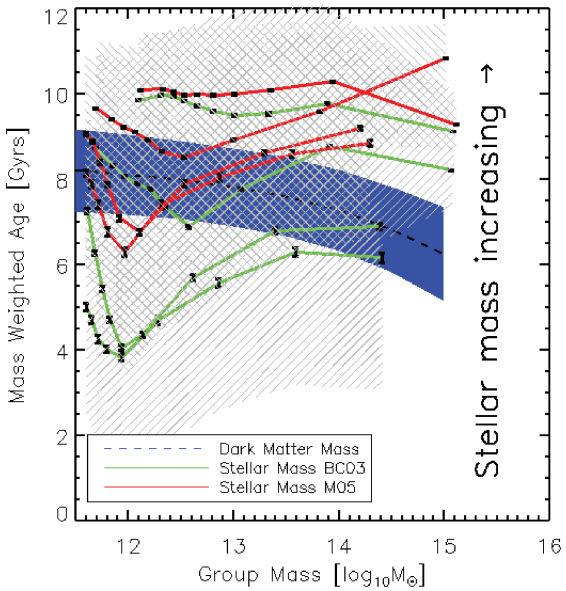

(d) Split by stellar mass

Figure 3. We show the dark matter assembly history, using the MAH code, and the assembly history in age bins reconstructed as could be measured with VESPA in Fig. 3(a). In Fig. 3(b) we show the stellar MWA as a function of halo mass, for galaxies from the semi-analytic models in the Millennium Simulation. Fig. 3(c) shows the stellar MWA as a function of group halo mass for both the M05 models (red) and BC03 models (green). We also show the dark matter MWA (DM MWA), as calculated by MAH code (black dotted lines) and show the 1σ dispersion on the dark matter MWA with the blue regions, which are determined by 10^4 random resamples using the bin ages available to VESPA. Fig. 3(d) is as Fig. 3(c) but we split the sample into fixed stellar mass bins M, which are given in units of $M_\odot$, by the ranges $10.2 \leq \log_{10} M < 10.4$, $10.4 \leq \log_{10} M < 10.8$, $10.8 \leq \log_{10} M < 11.2$ and $11.2 \leq \log_{10} M < 11.6$, and split the sample into bins of roughly equal number (as Fig. 2). Where applicable, we show the 1σ dispersion by the grey hashed region, and the error on the mean by the black error bars.

different stellar population models agree to within 1.5 Gyr and that the stellar MWA of most (60 to 90 per cent depending on stellar population model and galaxy sample) galaxies is older than 8 Gyr, independent of redshift, local galaxy density, dark matter halo mass or galaxy type. This is expected from the star formation history of the Universe, which peaks at around $z = 1$–2, corresponding to 8–10 Gyr look-back time (e.g. see Heavens et al. 2004).

We now return to the questions posed in the introduction.

(i) Does the stellar MWA depend on the local density?
(ii) Are similar trends seen in semi-analytic models?

To first order, we found that stellar MWA does not appear to be related to local galaxy density in either the observed or simulated data. We found similar dispersions in the observed and simulated

data and apparent flatness across local galaxy density (although see Cooper et al. 2010). We do find that the stellar MWA is strongly dependent on the total stellar mass of the galaxy.

(iii) Is the stellar MWA correlated with the mass of the Dark Matter Halo that the galaxy inhabits?

We did find a correlation of older stellar MWA with increasing dark matter halo mass in the observed galaxy sample, independent of stellar population model, which was also seen in the semi-analytic models, albeit for a smaller range in dark matter halo mass. By further splitting the sample into bins of total stellar mass, we identified that, as above, the stellar MWA is correlated with total stellar mass, but at second order the stellar MWA correlates with the host halo mass.

(iv) Is the stellar MWA correlated with the dark matter MWA?

We found that the dark matter MWA became anticorrelated with the stellar MWA as the mass of dark matter haloes increases. This is an observation of a 'downsizing' effect (Cowie et al. 1996) which describes the idea that the dark matter halo mass at which star formation is highest, shifts to lower masses at later times (see e.g. figs 8 and 9 of Conroy & Wechsler 2009; Jimenez et al. 2005). Another meaning of 'downsizing' is that more massive galaxies assembled more of their stars at higher redshift (and in a shorter time-scale) than less massive galaxies as seen in Fig. 2 and e.g. Thomas et al. (2005), Jimenez et al. (2007). These results have been seen previously by measuring the Specific SFRs (the amount of star formation per solar mass) of sets of similar mass galaxies over a range of redshifts.

Here, the downsizing effect is observed by the decrease in the stellar MWA as a function of decreasing stellar and dark matter halo mass, using VESPA stellar history reconstructions of the galaxy spectra. These conclusions are in agreement with other measures of 'downsizing' using MOPED to reconstruct the SFR histories of SDSS DR3 galaxies (Panter et al. 2007, found the SFR of massive galaxies peaked earlier than less massive galaxies).

We find VESPA is well suited for reconstructing stellar histories using the included synthetic stellar population models, and agrees well with semi-analytical models drawn from large simulations.

ACKNOWLEDGMENTS

The authors would like to thank Rita Tojeiro for VESPA data base support and useful suggestions, and Aday Robaina for insightful discussions and feedback which have improved the manuscript, and an anonymous referee whose suggestions improved the paper. BH would like to thank the Theory Division, Department of Physical Sciences, University of Helsinki for office space, and acknowledges funding from grant number FP7-PEOPLE- 2007- 4-3-IRG n 20218, LV is supported by FP7-PEOPLE-2007-4-3-IRG n. 202182, FP7-IDEAS-Phys.LSS 240117; LV and RJ are supported by MICINN grant AYA2008-03531. Funding for the SDSS and SDSS-II has been provided by the Alfred P. Sloan Foundation, the Participating Institutions, the National Science Foundation, the U.S. Department of Energy, the National Aeronautics and Space Administration, the Japanese Monbukagakusho, the Max Planck Society and the Higher Education Funding Council for England. The SDSS Web Site is http://www.sdss.org/.

REFERENCES

Abazajian K. et al., 2005, AJ, 129, 1755
Abazajian K. N. et al., 2009, ApJS, 182, 543
Adelman-McCarthy J. K. et al., 2006, ApJS, 162, 38
Bamford S. P. et al., 2009, MNRAS, 393, 1324
Blanton M. R. et al., 2005, AJ, 129, 2562
Boylan-Kolchin M., Springel V., White S. D. M., Jenkins A., Lemson G., 2009, MNRAS, 398, 1150
Bruzual G., Charlot S., 2003, MNRAS, 344, 1000 (BC03)
Conroy C., Wechsler R. H., 2009, ApJ, 696, 620
Cooper M. C., Gallazzi A., Newman J. A., Yan R., 2010, MNRAS, 402, 1942
Cooper M. C., Newman J. A., Madgwick D. S., Gerke B. F., Yan R., Davis M., 2005, ApJ, 634, 833
Cowie L. L., Songaila A., Hu E. M., Cohen J. G., 1996, AJ, 112, 839
Croton D. J. et al., 2006, MNRAS, 365, 11
De Lucia G., Blaizot J., 2007, MNRAS, 375, 2
De Lucia G., Kauffmann G., White S. D. M., 2004, MNRAS, 349, 1101
De Lucia G., Springel V., White S. D. M., Croton D., Kauffmann G., 2006, MNRAS, 366, 499
Eisenstein D. J. et al., 2001, AJ, 122, 2267
Ferreras I., Pasquali A., Rogers B., 2010, (arXiv:1012.0310)
Gallazzi A., Charlot S., Brinchmann J., White S. D. M., Tremonti C. A., 2005, MNRAS, 362, 41
Górski K. M., Hivon E., Banday A. J., Wandelt B. D., Hansen F. K., Reinecke M., Bartelmann M., 2005, ApJ, 622, 759
Graff P., Hobson M., Lasenby A., 2011, MNRAS, 413, L66
Heavens A., Panter B., Jimenez R., Dunlop J., 2004, Nat, 428, 625
Heavens A. F., Jimenez R., Lahav O., 2000, MNRAS, 317, 965
Jimenez R., Panter B., Heavens A. F., Verde L., 2005, MNRAS, 356, 495
Jimenez R., Bernardi M., Haiman Z., Panter B., Heavens A. F., 2007, ApJ, 669, 947
Maraston C., 2005, MNRAS, 362, 799 (M05)
Maraston C., Strömbäck G., Thomas D., Wake D. A., Nichol R. C., 2009, MNRAS, 394, L107 (M05)
Mateus A., Jimenez R., Gaztañaga E., 2008, ApJ, 684, L61
Noeske K. G. et al., 2007a, ApJ, 660, L43
Noeske K. G. et al., 2007b, ApJ, 660, L47
Panter B., Jimenez R., Heavens A. F., Charlot S., 2007, MNRAS, 378, 1550
Pasquali A., Gallazzi A., Fontanot F., van den Bosch F. C., De Lucia G., Mo H. J., Yang X., 2010, MNRAS, 407, 937
Schlegel D. J., Finkbeiner D. P., Davis M., 1998, ApJ, 500, 525
Schmidt M., 1968, ApJ, 151, 393
Springel V., 2005, MNRAS, 364, 1105
Springel V. et al., 2005, Nat, 435, 629
Springel V., Yoshida N., White S. D. M., 2001, Nat, 6, 79
Strauss M. A. et al., 2002, AJ, 124, 1810
Thomas D., Maraston C., Bender R., Mendes de Oliveira C., 2005, ApJ, 621, 673
Tojeiro R., Heavens A. F., Jimenez R., Panter B., 2007, MNRAS, 381, 1252
Tojeiro R., Percival W. J., Heavens A. F., Jimenez R., 2011, MNRAS, 413, 434
Tojeiro R., Wilkins S., Heavens A. F., Panter B., Jimenez R., 2009, ApJS, 185, 1
Yang X., Mo H. J., van den Bosch F. C., Pasquali A., Li C., Barden M., 2007, ApJ, 671, 153
York D. G. et al., 2000, AJ, 120, 1579
Zhao D. H., Jing Y. P., Mo H. J., Börner G., 2009, ApJ, 707, 354

This paper has been typeset from a TEX/LATEX file prepared by the author.